

Theoretical and Practical Study of a Photovoltaic MPPT Algorithm Applied to Voltage Battery Regulation

Sihem Amara*, Adel Bouallegue**[‡], Adel Khedher*

* Laboratory of Renewable Energy and Electrical Vehicles Laboratory, National Engineering School of Sfax, Sfax, Tunisia

** Laboratory of Advanced Systems in Electrical Engineering, National Engineering School of Sousse, Sousse, Tunisia

(sihem.amara@gmail.com, adel.bouallegue@eniso.rnu.tn, adel_khedher@yahoo.fr)

[‡]Corresponding Author; Adel Bouallegue, BP 267, 4023 Riadh City, Sousse, Tunisia, Tel: (+216) 20308976,
Fax: (+216) 73369506, adelbouallegue@gmail.com

Received: 09.12.2013 Accepted: 22.02.2014

Abstract- The energy produced by the photovoltaic systems is very intermittent and depends enormously on the weather conditions. This is why it is important to find a way to store this energy. This paper proposes a design and implementation of a photovoltaic power generation system controller. As to extract maximum power from the PV panel, the proposed system controls both the boost converter and the battery charger using a microcontroller. The proposed solution is based on the PIC16F877 microcontroller. Experimental results, based on the MCU are agreed with the Matlab/Simulink simulation.

Keywords- Microcontroller, MPPT, Perturb and Observe, Photovoltaic, Regulator of charge.

1. Introduction

In recent years, the petroleum is getting more and more expensive. So that the people look for new green energy, as solar, wind, water, etc. Nowadays, we can use photovoltaic sources in many applications like water pumping, battery charging, etc [1]. Energy provides by the sun is a neat, maintenance-free, clean and an abundant resource of nature, so it is suitable to be a green energy source. But, there are still some disadvantages as follow: the install cost of solar panels is high, and the conversion efficiency is still lower [2].

The current/voltage curves of photovoltaic characteristic depend primarily on the level of illumination of the cells and their temperature. Each solar module has a single optimal operating point, called the maximum power point (MPP) which changes with its own characteristic as good as cell temperature and sunlight [3]. These dependencies on climate behaviour make it difficult to keep the MPP operating when the curve of power/voltage is varying. To resolve this problem, many maximum power point of solar module tracking (MPPT) algorithms were proposed in lecture [4]. These algorithms have been an active research subject over the past few years growing with the people interest in renewable. Some of the widely used algorithms are the hill climbing methods [5], the incremental conductance method

[6], and the ripple based method [7] and the constant voltage method [8].

These techniques differ in many sides including, hardware implementation, simplicity, cost range of the effectiveness, convergence speed, sensors required, and needs for parameterization [9].

In this work, we have realized a standalone photovoltaic generator composed by a photovoltaic module, a charge regulator, storage battery and a load. The function of the charge regulator is to control the battery charge/discharge avoiding its damage by preventing overcharging and excessive discharging[10].The regulator is controlled the duty cycle calculated by the MCU according to the MPPT algorithm [11].The studied system diagram is depicted in Fig.1.

In the second section, we present the modelling of each bloc of the system. Then, implementations in Matlab/Simulink environment and simulation results are shown in the third section. Finally, experimental results using the MCU are presented and discussed in section 4.

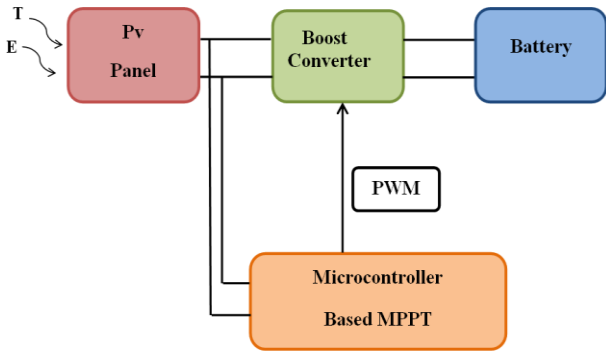


Fig. 1.Block diagram of the battery voltage regulator with MPPT.

2. Modelling of the Studied System

2.1 The PV Module

The principle of a photovoltaic cell is to convert sunlight energy into electricity. It is fundamentally a p-n semiconductor junction diode. The simplest equivalent circuit of the PV cell is shown in Fig. 2. It is composed of a photo current, a diode, a series resistor, and a parallel resistor.

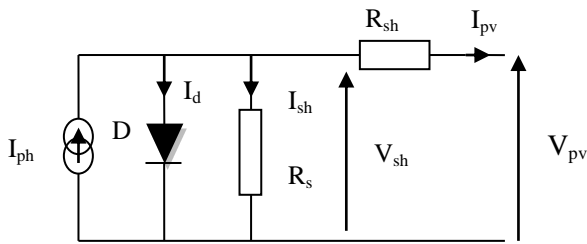


Fig. 2. Equivalent circuit of a photovoltaic cell.

A photovoltaic panel (PVP) is constituted of N_p parallel modules each one including N_s serial-connected PV cells [12]. The basic equation of PV panel model is given by Eq. (1).

$$I_{pv} = N_p I_{ph} - N_p I_s \left(\exp \left(\frac{V_{pv} + I_{pv} R_s}{N_s} \frac{q}{kTA} \right) - 1 \right) - \frac{\left(\frac{N_p V_{pv}}{N_s} + I_{pv} R_s \right)}{R_{sh}} \quad (1)$$

The cell's saturation current I_s is related to the temperature T as follow:

$$I_s = I_{rs} \left(\frac{T}{T_{ref}} \right)^3 \exp \left[\frac{qE_g}{kqA} \left(\frac{1}{T_{ref}} - \frac{1}{T} \right) \right] \quad (2)$$

I_{rs} is defined as cell reverse saturation current, it changes with temperature according to the following equation:

$$I_{rs} = \frac{I_{sc}}{\left[\exp \left(\frac{qV_{oc}}{kTA} \right) - 1 \right]} \quad (3)$$

As far as, the photocurrent I_{ph} depends on the solar

radiation E the cell temperature T :

$$I_{ph} = \frac{E}{E_{ref}} \left[I_{ph} + k_i (T - T_{ref}) \right] \quad (4)$$

Based on the mathematical model described by the different equations mentioned above, we can realize the Simulink model as shown in Fig. 3.

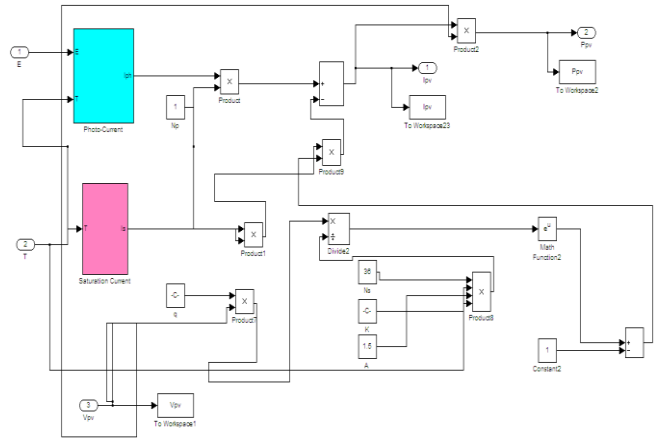


Fig. 3. Model Simulink of PV Panel.

2.2 Maximum power point tracker using Perturb and Observe method (P&O)

The characteristic of a PV generator depends on fluctuations of the array temperature and irradiance. Hence, there is a need to persistently track the power-voltage profile, and maintain the solar panel operating voltage at the point where the maximum power is extracted. We called this process the maximum power point tracking [13].

Many control algorithms for MPPT have been proposed in the literature. Two algorithms often used to achieve the MPPT are [14]: the P&O method and the incremental conductance method.

The P&O algorithm can be also named ‘‘Hill-Climbing’’. Both these names mean the same algorithm but the difference between them is the way of their implementation. Hill-climbing is implied to a perturbation on the output PV power P_{pv} , while the P&O algorithm uses not only P_{pv} but also the voltage perturbation V_{pv} and this is the technique chosen in this work to implement the MPPT control algorithm regarding its simplicity, and the possibility to introduce ameliorations in the energy storage process [15]. Furthermore, it is nowadays, the most commonly used MPPT algorithm in commercial PV products.

In this method, the last perturbation is used to forecast the next perturbation value. The principle of P&O is based on evaluating the perturbation by decreasing or increasing the duty cycle, and then observing the P_{pv} variation. The algorithm flowchart is presented in Fig. 4 [16] [17].

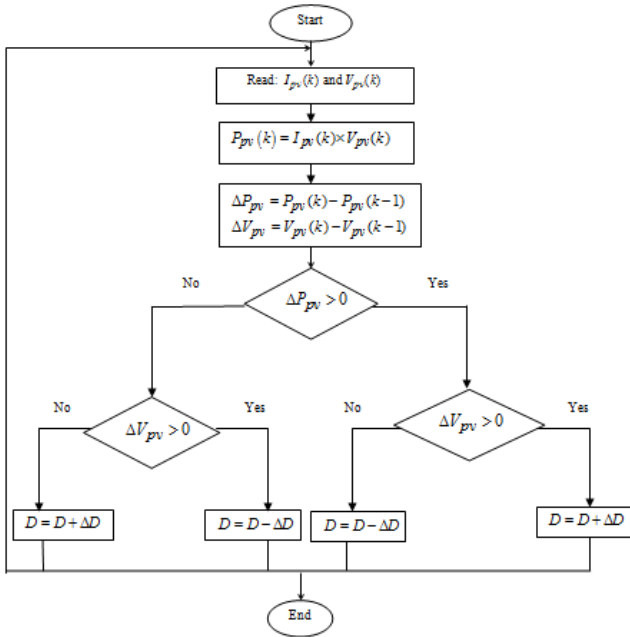


Fig. 4. Flow chart of P&O method.

2.3 Boost Convertor

A boost converter can be also called in the literature as the step-up converter because the DC voltage output is higher than its DC voltage input. It is a sort of power converter, which is composed by two semiconductor switches (a diode and a switch or transistor) and one energy storage element [18]. It is controlled periodically with a modulation period T. Over this period, t_{off} called the closing time and t_{on} the opening time, we have: $T = t_{on} + t_{off}$. The duty cycle of the converter is defined as: $\alpha = \frac{t_{off}}{T}$ which is also called D.

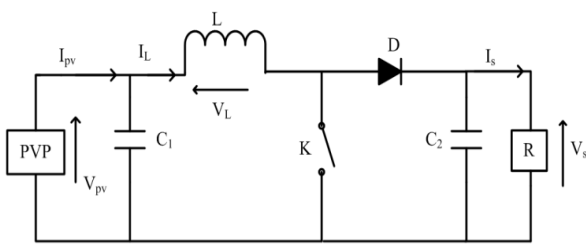


Fig. 5. Boost converter design.

The operation principle of the boost converter can be described by two modes:

- First mode: K=1, D=0

$$\begin{cases} V_{pv} = L \frac{dI_L}{dt} \\ \frac{dV_s}{dt} = -\frac{1}{RC_2} V_s \\ I_{pv} = I_L + C_1 \frac{dV_{pv}}{dt} \\ \frac{I_s}{I_{pv}} = 1 - \alpha \end{cases} \quad (5)$$

$$\dot{X} = A_1 X + B_1 U \text{ With } X = \begin{bmatrix} I_L \\ V_s \\ V_{pv} \end{bmatrix} \text{ and } U = \begin{bmatrix} I_{pv} \\ I_s \\ V_{pv} \end{bmatrix} \quad (6)$$

$$\begin{bmatrix} \frac{dI_L}{dt} \\ \frac{dV_s}{dt} \\ \frac{dV_{pv}}{dt} \end{bmatrix} = \begin{bmatrix} 0 & 0 & \frac{1}{L} \\ 0 & -\frac{1}{RC_2} & 0 \\ -\frac{1}{C_1} & 0 & 0 \end{bmatrix} \begin{bmatrix} I_L \\ V_s \\ V_{pv} \end{bmatrix} + \begin{bmatrix} 0 & 0 & 0 \\ 0 & 0 & 0 \\ \frac{1}{C_1} & 0 & 0 \end{bmatrix} \begin{bmatrix} I_{pv} \\ I_s \\ V_{pv} \end{bmatrix} \quad (7)$$

- Second mode: K=0, D=1

$$\begin{cases} V_{pv} - V_s = L \frac{dI_L}{dt} \\ C_2 \frac{dV_s}{dt} = I_L - \frac{V_s}{R} \\ I_{pv} = C_2 \frac{dV_{pv}}{dt} \\ \frac{V_s}{V_{pv}} = \frac{1}{1 - \alpha} \end{cases} \quad (8)$$

$$\dot{X} = A_2 X + B_2 U \text{ With } X = \begin{bmatrix} I_{pv} \\ I_s \\ V_{pv} \end{bmatrix} \text{ And } U = \begin{bmatrix} I_L \\ V_s \\ V_{pv} \end{bmatrix} \quad (9)$$

$$\begin{bmatrix} \frac{dI_L}{dt} \\ \frac{dV_s}{dt} \\ \frac{dV_{pv}}{dt} \end{bmatrix} = \begin{bmatrix} 0 & -\frac{1}{L} & \frac{1}{L} \\ \frac{1}{C_2} & -\frac{1}{RC_2} & 0 \\ 0 & 0 & 0 \end{bmatrix} \begin{bmatrix} I_L \\ V_s \\ V_{pv} \end{bmatrix} + \begin{bmatrix} 0 & 0 & 0 \\ 0 & 0 & 0 \\ \frac{1}{C_1} & 0 & 0 \end{bmatrix} \begin{bmatrix} I_{pv} \\ I_s \\ V_{pv} \end{bmatrix} \quad (10)$$

By using equations defined previously we can lead to the model average state of boost:

$$\dot{X} = AX + BU \text{ With: } \begin{cases} A = A_1 \alpha + A_2 (1 - \alpha) \\ B = B_1 \alpha + B_2 (1 - \alpha) \end{cases} \quad (11)$$

And

$$A = \begin{bmatrix} 0 & 0 & \frac{1}{L} \\ 0 & -\frac{1}{RC_2} & 0 \\ -\frac{1}{C_1} & 0 & 0 \end{bmatrix} \alpha + \begin{bmatrix} 0 & -\frac{1}{L} & \frac{1}{L} \\ \frac{1}{C_2} & -\frac{1}{RC_2} & 0 \\ 0 & 0 & 0 \end{bmatrix} (1-\alpha)$$

$$B = \begin{bmatrix} 0 & 0 & 0 \\ 0 & 0 & 0 \\ \frac{1}{C_1} & 0 & 0 \end{bmatrix} \alpha + \begin{bmatrix} 0 & 0 & 0 \\ 0 & 0 & 0 \\ \frac{1}{C_1} & 0 & 0 \end{bmatrix} (1-\alpha)$$

Finally we have:

$$\begin{cases} \frac{dI_L}{dt} = \frac{V_{pv}}{L} - \frac{V_s}{L}(1-\alpha) \\ \frac{dV_s}{dt} = \frac{I_L}{C_2}(1-\alpha) - \frac{1}{RC_2}V_s \\ \frac{dV_{pv}}{dt} = \frac{1}{C_1}(I_{pv} - I_L) \end{cases} \quad (12)$$

2.4 The MPPT Charge Regulator

In order to charge the battery with the maximum power, the suggested control circuit compels the system to run to its optimal operating point within variable temperature and irradiation conditions. This regulator is shown in Fig. 6. The main role of the MPPT algorithm is to modify the duty cycle of the boost until reaching the maximum power point [19].

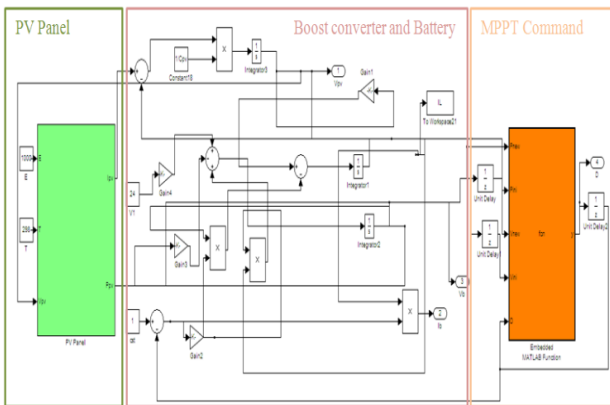


Fig. 6. Model Simulink of the regulator charger.

The battery used in this work has the model described in Fig.7 which can be characterized by the following equation [20]:

$$V_b = V_1 - R_b I_b \quad (13)$$

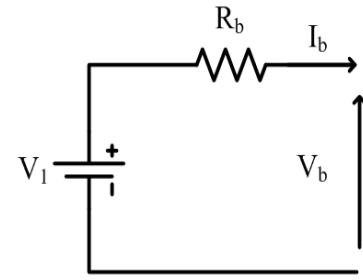


Fig. 7. Battery model.

In block Boost converter and battery, the equations below where used:

$$\begin{cases} \frac{dI_L}{dt} = \frac{V_{pv}}{L} - \frac{V_b}{L}(1-\alpha) \\ \frac{dV_b}{dt} = \frac{I_L}{L}(1-\alpha) - \frac{1}{R_b C_2}V_b + \frac{1}{R_b C_2} \\ \frac{dV_{pv}}{dt} = \frac{1}{C_1}(I_{pv} - I_L) \end{cases} \quad (14)$$

To find these equations we had followed the same steps described in the section 2.3 except that the resistance R is replaced by the equation of the battery.

3. Results and Discussion

3.1 Simulation of the PV panel

The developed model of PVP is simulated for different solar insolation and different temperature level. The parameters of this developed model are given in Table 1. Simulation results are demonstrated in Fig.8 and Fig. 9. These figures show that with increasing temperature, the Open circuit voltage \$V_{oc}\$ of the PVP and the maximum power output decrease while the Short circuit current \$I_{sc}\$ increases. On the other hand, with increasing of solar insolation the \$I_{sc}\$ of the PV module increases and the maximum power output increases as well. The reason is that \$I_{sc}\$ is directly related to the radiant intensity, yet the \$V_{oc}\$ is logarithmically dependent on the solar irradiance [21].

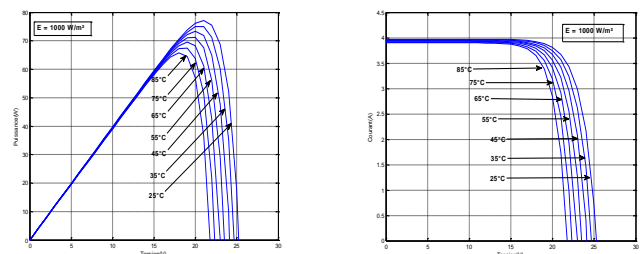


Fig. 8. Characteristic curves (\$P_{pv}\$-\$V_{pv}\$) and (\$I_{pv}\$-\$V_{pv}\$) at different module working temperature.

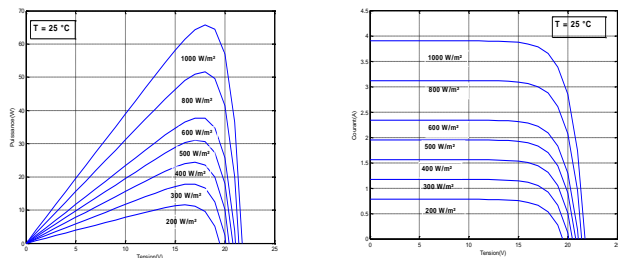


Fig. 9. Characteristic curves (P_{pv} - V_{pv}) and (I_{pv} - V_{pv}) at different insulation level.

The point of maximum power is the desired operating point for a photovoltaic array to obtain maximum efficiency. The corresponding values for voltage and current at maximum power are respectively called V_{mp} and I_{mp} , respectively [22].

3.2 Perturb and Observe Simulation Results

In this section we describe the simulation results of the isolated PV system using the P&O algorithm. Parameters are set as follow:

$$L=0.03 \text{ H}; C1=0.001 \text{ F}; C2=0.000068 \text{ F}; R=30 \ \Omega.$$

The simulation results illustrated in Fig.10 show the growing of the V_{pv} value, as well as the I_{pv} and P_{pv} variations. V_{pv} begins from zero and raises by 0.01 V on every perturbation cycle. I_{pv} starts from I_{sc} and decreases until the power reached the maximum.

We can see that:

- The MPPT control oscillates the operating point around the MPP, after a transitional period of time equal nearly 100 ms.
- The different electrical variables whatever P_{pv} , V_{pv} and I_{pv} stabilize around values that we have set:
- The P_{pv} stabilizes around 68 W and that the output of the converter P_s around 80 W.
- At the output of the panel, the V_{pv} and I_{pv} respectively stabilize around 21.7 V and 3.9 A.
- At the output of the boost, the voltage V_s and current I_s stabilize respectively around 32 V and 2.5A.

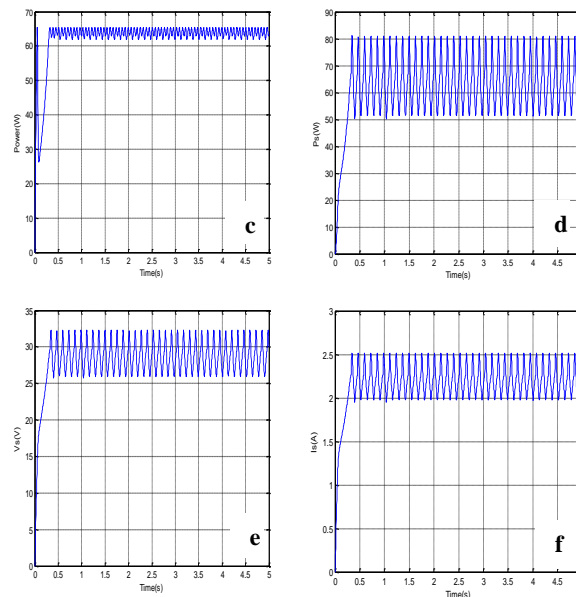
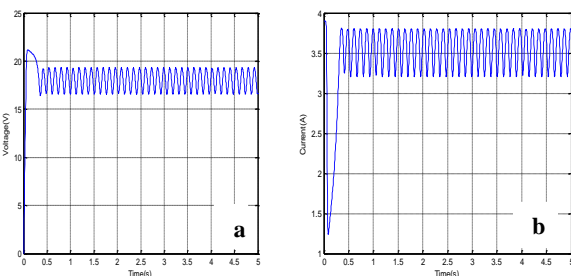


Fig. 10. Variation of V_{pv} (V)(a), I_{pv} (A)(b) , P_{pv} (W) (c), P_s (W), V_s (V) and I_s (A).

All obtained results show that the DC / DC converter and the MPPT control are a good choice and an efficient solution to adapts the PV generator to the load R in order to transfer the maximum power supplied by the PV generator.

3.3 Simulation of the proposed system with illumination variation

Fig. 11 illustrates the simulation results of the proposed system applying an arbitrarily solar irradiance .Simulation are made with different values of E respectively 800W/m², 878 W/m², 400 W/m², 900 W/m², 300 W/m².

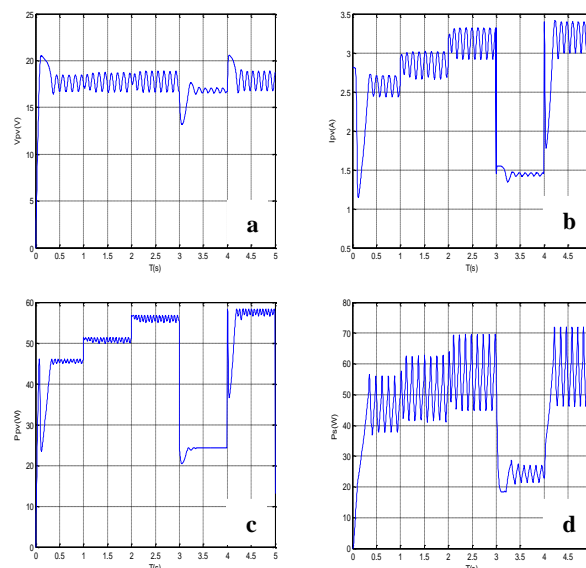


Fig. 11. Simulation of V_{pv} (V) (a), I_{pv} (A) (b), P_{pv} (W) (c) and P_s (W) (d) under a variable illumination.

3.4 Simulation of the Proposed System with Temperature Variation

Fig. 12 illustrates the simulation results of the proposed system changing this time arbitrarily the temperature. Simulation are made with different values of T respectively 298 ° K, 328 ° K, 358 ° K, 338 ° K, 308 ° K, 348 ° k, 328 ° k.

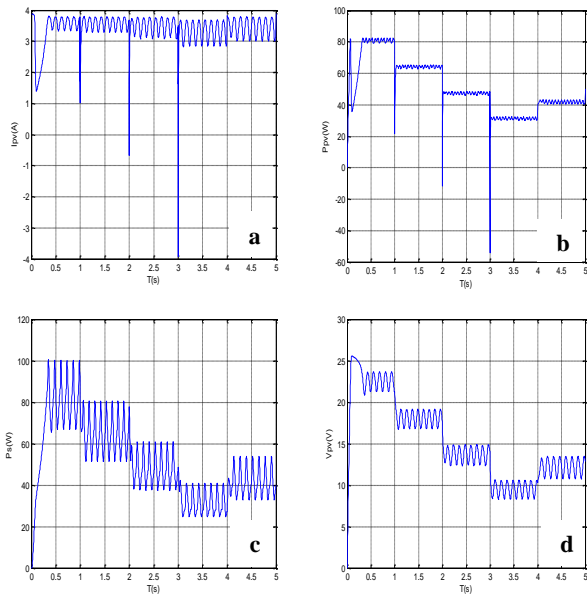


Fig. 12. Simulation of I_{pv}(A) (a), P_{pv}(w) (b), P_s(W) (c) and V_{pv}(V) (d) under a variable temperature.

Another result shows that the efficiency of the developed algorithm is illustrated by the figure below Fig.13. We note that D varies with the variation of insolation and temperature. This simulation has also clearly demonstrated the influence of the developed Mppt algorithm on the I_{pv}-V_{pv} and P_{pv}-V_{pv} curves. We remark that by changing either the temperature or insolation, the system can always track the maximum power point.

So,we can note that the MPPT algorithm based on the principle P & O algorithm is robust and is able to easily follow the maximum power point.

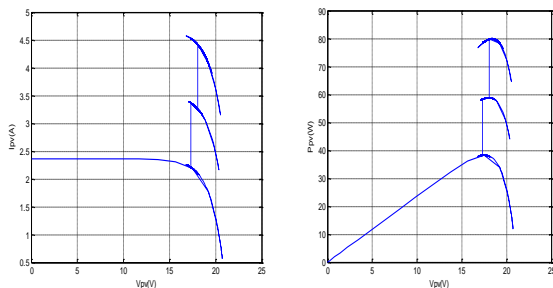


Fig. 13. Influence of MPPT on I_{pv} (V_{pv}) and P_{pv}(V_{pv}) curve

3.5 Simulation of the MPPT Regulator

In this section, we present simulation results of the voltage regulator obtained by using Matlab/Simulink.

Profiles of P_{pv}, V_{pv}, V_b and I_b with time variation are presented in Fig. 14. Parameters of the battery are set as follow: V₁=24V and R_b=0.1Ω.

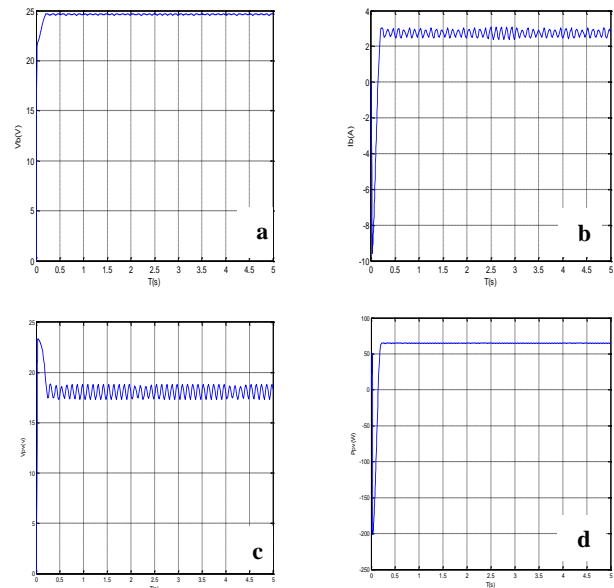


Fig. 14.Variation of Voltage V_b (a), current I_b (b), V_{pv} (c) and Power P_{pv}.

After simulation of the MPPT that the system is stable. The switching action of the dc-dc converter causes oscillations at the optimal operating point. Also,we can affirm that the applied of MPPT algorithms in battery charging proposes evidently benefits to the life duration of the battery. If you compare this process to direct connection, we can note that the absorbed power from the PVP has been ameliorated from 30% to 50% [23].

4. Implementation on Microcontroller

The overall system block diagram, implemented in ISIS software, consists of PV panel, charge controller, battery and LCD displayer is described in Fig 15. The PIC sets the duty cycle using Hill climbing method to allow the solar modules to operate at their maximum power point transmitted to the battery.

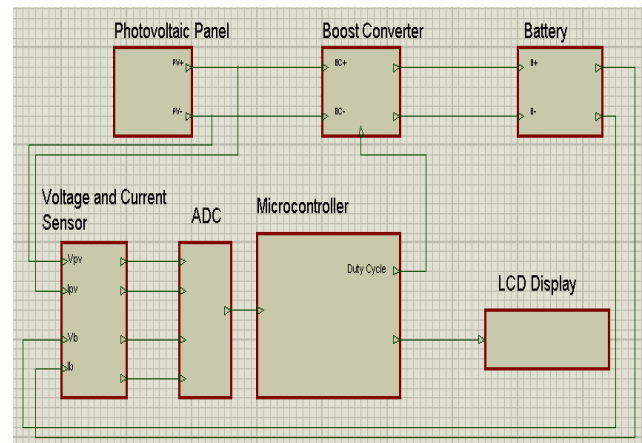


Fig. 15. Block Diagram of MPPT Charge Controller Circuit.

Current sensors deliver the current to the microcontroller through the digital converter (ADC) [24]. The value of the V_{pv} , I_{pv} , P_{pv} , V_b , I_b and duty cycle D initialized to 0.5 are well measured and displayed on the LCD.

The DC-DC converter circuit consists of MOSFETs which are made to control the power, by the driving square wave signals at the gate.

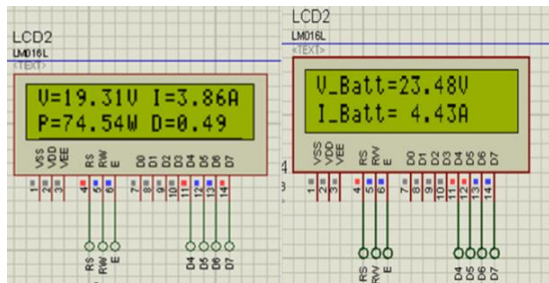


Fig. 16. Display of P_{pv} , V_{pv} , I_{pv} , D , I_b and V_b

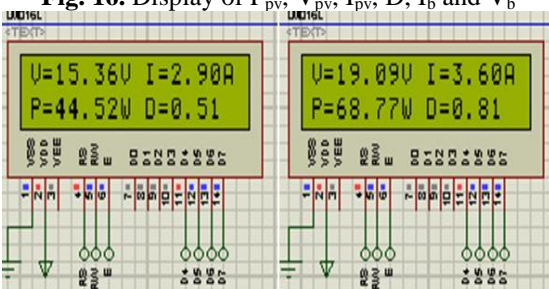


Fig. 17. Operation of Hill Climbing algorithm: increase of power results causes the increase of the duty cycle

5. Conclusion

In this paper, we have presented the principle of the PV cell and their mathematical model. A Matlab/Simulink simulation of the model helped us to prove that the GPV is highly depend on weather condition essentially the temperature and illumination [25]. Besides, an MPPT algorithm has been presented to detect the maximum of power and transfer it to the load; this method has been practically implemented using a microcontroller. The selected control algorithm based on the P&O maximum power point tracking function, enabling the transfer of maximum energy generated by the PVP to the battery. Moreover, this algorithm can provide an efficient specific and reliable maximum power tracking performance even under a rapidly changing in irradiance and temperature condition. Simulation results show that the MPPT stand alone system is more efficient than a simple direct connection.

Nomenclature

- K: the Boltzmann constant ($1.3806503 \times 10^{-23}$ J/K).
- q: the electron charge ($1.60217646 \times 10^{-19}$ C).
- Rsh: Parallel resistance of cell, Ω .
- Rs: Series resistance of cell, Ω .

References

- [1] M. A. S. Masoum, S. M. M. Badejani, and E. F. Fuchs, "Microprocessor-controlled new class of optimal battery chargers for photovoltaic applications," *IEEE Trans. Energy Convers.*, Vol. 19, No. 3, pp. 599–606, Sep. 2004
- [2] K. K. Tse, B. M. T. Ho, H. S.-H. Chung, and S. Y. R. Hui, "A comparative study of maximum-power-point trackers for photovoltaic panels using switching-frequency modulation scheme," *IEEE Trans. Ind. Electron.*, vol. 51, no. 2, pp. 410–418, Apr. 2004.
- [3] Salas, V., A. Barrado, E. O., Lazaro, A. (2006). Review of the maximum power point tracking algorithms for stand-alone photovoltaic systems. *Solar Energy Materials & Solar Cells*, Vol.90, pp: 1555–1578.
- [4] S. Chin, J. Gadson, and K. Nordstrom, "Maximum Power Point Tracker," *Tufts University Department of Electrical Engineering and Computer Science*, 2003, pp.1-66.
- [5] N. Femia, G. Petrone, G. Spagnuolo, and M. Vitelli, "Optimization of perturb and observe maximum power point tracking method," *IEEE Trans. Power Electron*, Vol.20, No. 4, pp. 963–973, Jul. 2005.B.
- [6] J. Young-Hyok, J. Doo-Yong, K. Jun-Gu, K. Jae-Hyung, L. Tae-Won, and W. Chung-Yuen, "A Real Maximum Power Point Tracking Method for Mismatching Compensation in PV Array Under Partially Shaded Conditions," *Power Electronics, IEEE Transactions on*, Vol. 26, No. 4, pp. 1001-1009, 2011.
- [7] Yang Du, «Battery-integrated boost converter utilizing distributed MPPT configuration for photovoltaic systems», *Solar Energy*, NO 85, pp. 1992–2002, 2011.
- [8] S. Balakrishna, Thansoe, Nabil A., Rajamohan G., Kenneth A. S., Ling C. J., "The Study and Evaluation of Maximum Power Point Tracking Systems," *International Conference on Energy and Environment 2006 (ICEE)*, pp. 17-22, 2006.
- [9] R. F. Coelho, F. M. Concer, D. C. Martins "A Simplified Analysis of DC-DC Converters Applied as Maximum Power Point Tracker in Photovoltaic Systems" *IEEE international symposium on power electronics for distributed generation systems*.
- [10] M. Lokanadham, «Incremental Conductance based Maximum Power Point Tracking (MPPT) for Photovoltaic System», *International Journal of Engineering Research and Applications (IJERA)*, Vol. 2, Issue 2, pp. 1420-1424, 2012.
- [11] J. L. Yang, « Research on MPPT and Single-Stage Grid-Connected For Photovoltaic System», *Wseas transactions on systems*, issue 10, Vol. 7, pp. 1117–1130, October 2008
- [12] N. A. Kelly, T. L. Gibson, «Solar photovoltaic charging of high voltage nickel metal hydride batteries using DC power conversion», *Journal of Power Sources*, Vol. 196, pp. 10430–10441, 2011

- [13] S. H. Ko, «Photovoltaic dynamic MPPT on a moving vehicle», Solar Energy, Vol 86, pp.1750–1760, 23 April 2012.
- [14] M. Garcia, « Experimental study of mismatch and shading effects in the I-V characteristic of a photovoltaic module », Solar Energy Materials & Solar Cells, Vol 90, Issue 3, pp. 329–340, 15 February 2006.
- [15] Y. H. Liu, «A fast and low cost analog maximum power point tracking method for low power photovoltaic systems», Solar Energy, No 43, pp.2771 2780,September 2011.
- [16] D. Ganesh, «A Voltage Controller in photovoltaic System with Battery Storage for Stand-Alone Applications», International Journal of Power Electronics and Drive System (IJPEDS), Vol 2, No 1, pp. 9-18, Mars 2012.
- [17] R. Gules, «A Maximum Power Point Tracking System with parallel connection for PV Stand-Alone Applications», IEEE, Vol. 55, NO. 7, July 2008.
- [18] T. Bennett, «Photovoltaic model and converter topology considerations for MPPT purposes», Solar Energy, pp.2029–2040, May 2012.
- [19] T. ESRAM, «Comparison of Photovoltaic Array Maximum Power Point Tracking Techniques», IEEE, VOL: 22, NO. 2, June 2007.
- [20] Y. Yongchang, «Implementation of a MPPT Controller Based on AVR Mega16 for Photovoltaic Systems», Energy Procedia, pp. 241 – 248, 2012.
- [21] F. Chekired, « Implementation of a MPPT fuzzy controller for photovoltaic systems on FPGA circuit», Energy Procedia, Vol 6, pp.541–54, 2011.
- [22] N. Karamia, «Analysis and Implementation of an adaptive PV based battery floating Charger», Solar Energy, Vol 86, pp. 2383–2396, 2012.
- [23] T. N. Khatib, «A New Controller Scheme for Photovoltaics Power Generation System », European Journal of Scientific Research, Vol.33 No.3, pp. 15-524, 2009.
- [24] M. A. E. Galdino, C. M. Ribeiro, “A Intelligent Battery Charge Controller for Small Scale PV Panel”, 12th European Photovoltaic Solar Energy Conference and Exhibition, 1994.

Annex

Electrical characteristics of the photovoltaic module

Electrical Characteristics (STC)	Abbreviation	Value
Band-gap energy of the	E_g	1.2 eV
The diode ideality constant	A	1.5
Maximum power	P_{max}	65.7 W
Voltage at Pmax	V_{mp}	18 V
Current at Pmax	I_{mp}	3.65 A
Open circuit voltage	V_{oc}	21.7 V
Short circuit current	I_{sc}	3.9 A
Temperature coefficient of I_{sc}	K_i	1.2mA/°C
Number of cells in parallel	N_p	1
Number of cells in series	N_s	36